Sand dune mobility under climate change in the Kalahari and Australian deserts

Y. Ashkenazy, H. Yizhaq & Haim Tsoar

Climatic Change
An Interdisciplinary, International Journal Devoted to the Description, Causes and Implications of Climatic Change

ISSN 0165-0009
Volume 112
Combined 3-4

Climatic Change (2012) 112:901-923
DOI 10.1007/s10584-011-0264-9

Springer

Climatic Change (2012) 112:901–923
DOI 10.1007/s10584-011-0264-9

Sand dune mobility under climate change in the Kalahari and Australian deserts

Y. Ashkenazy · H. Yizhaq · Haim Tsoar

Received: 24 June 2009 / Accepted: 31 August 2011 / Published online: 11 October 2011

Abstract Vegetation cover on sand dunes mainly depends on wind power (drift potential—DP) and precipitation. When this cover decreases below a minimal percentage, dunes will start moving. It is therefore necessary to study the effects of DP and precipitation on contemporary dune activity in order to predict likely future dune mobility in the coming decades. We concentrate on the future activity of the currently fixed dune fields of the Kalahari and the Australian deserts. These sand seas include the largest areas of stabilized dunes in the world, and changes in their mobility have significant economic implications. Global maps of DP are introduced, based on real and reanalysis data. Analyses of two global circulation models (GFDL and CGCM3.1) provide future predictions under the SRES-A1B IPCC scenario, which is a moderate global warming scenario. According to the GFDL model, both the Australian and Kalahari basin dunes will apparently remain stable towards the end of the 21st century because the DP will stay small, while the rate of precipitation is expected to remain much above the minimal threshold necessary for the vegetative growth that leads to dune stabilization. The CGCM model predicts insignificant changes in DPs and shows that the precipitation rate is above 500 mm/year for almost the entire Kalahari basin. The central-northern part of Australia is predicted to have larger DPs and greater precipitation than the southern part. Since the predicted changes in DP and precipitation are generally not drastic, both the Australian desert and Kalahari basin dunes are not likely to become active. Still, the Australian dunes are more likely to remobilize than the Kalahari ones due to some decrease in precipitation and an increase in wind power.

Y. Ashkenazy (✉) · H. Yizhaq
Department of Solar Energy and Environmental Physics, The J. Blaustein Institutes for Desert Research, Ben Gurion University of the Negev, Sede Boker Campus 84990, Israel
e-mail: ashkena@bgu.ac.il

H. Tsoar
Department of Geography and Environmental Development, Ben-Gurion University of the Negev, Beer-Sheva, Israel

1 Introduction

Sand dunes cover vast land areas and are located primarily in arid regions. These large sand seas are concentrated in Africa, Australia, and Asia (Fig. 1), with about half of them exhibiting stable, fixed configurations. Most of the currently fixed dunes were active during the last glacial maximum (e.g., Hesse et al. 2003; Fitzsimmons et al. 2007a, b; Stone and Thomas 2008) when the weather was colder and drier and air turbulence was stronger (e.g., Harrison et al. 2001; Lunt and Valdes 2001, 2002; Duller and Augustinus 2006). One factor modulating and weakening wind action on sand is vegetation (Wasson and Nanninga 1986; Buckley 1987; Wolfe and Nickling 1993; Buckley 1996; Hugenholtz and Wolfe 2005; Okin 2008), whose growth can lead to dune stabilization. Therefore, when precipitation is too low to support vegetation, dunes may be reactivated (Tsoar 2005). Several indications of dune reactivation have been reported in the past decades (e.g. Muhs and Maat 1993; Thomas et al. 2005; Alexander 2007).

Geomorphologists usually characterize dune mobility in terms of mobility indexes (e.g., Wasson 1984; Talbot 1984; Lancaster 1988; Tsoar 2005), which are considered to depend on climatological parameters, such as precipitation, temperature, (potential) evapotranspiration, and wind speed. However, dune dynamics are much more complicated and involve various self-interacting processes that cannot be modeled by simple diagnostic indexes. The recently reported coexistence of fixed and active dunes under similar climatic conditions demonstrates the limitation of dune-stability indexes (Tsoar 2005; Yizhaq et al. 2007, 2009). Moreover, this bi-stability seems to be related to a hysteresis phenomenon in which dunes experience abrupt, fixed-to-active state transitions when a particular climatic parameter reaches a critical value (Yizhaq et al. 2007, 2009). Thus, a future change in a dune's dynamic state may be generally estimated by examining changes in the size of climatic parameters: large changes in a relevant climatic parameter are more likely to push the dunes beyond their fixed-to-active (or active-to-fixed) transition point.

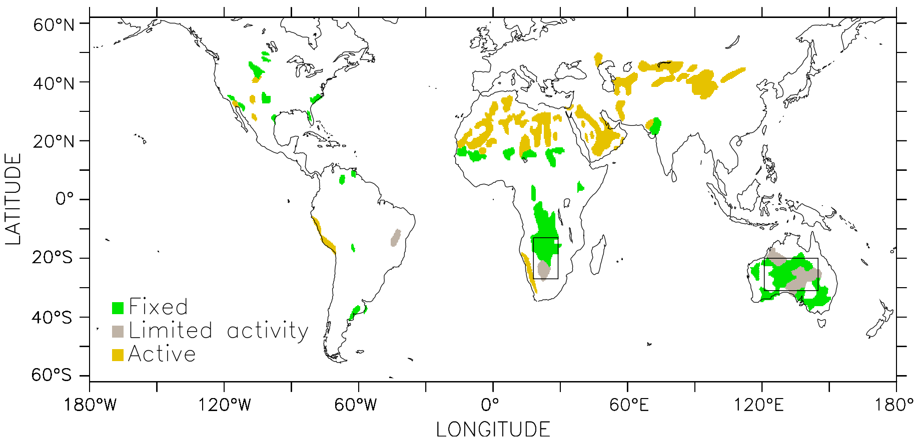

Fig. 1 A map of the world's dune areas, divided into active (*yellow*), limited activity (*gray*), and fixed (*green*) regions. The map is based on the approximated sand seas map of Thomas (1997). The *rectangles* indicate the areas whose properties are summarized in Fig. 11. Note that most of the dunes of central Asia are currently stable although they are indicated as active according to Thomas (1997). Also note that only the southern part of the Kalahari basin is indicated as the northern part has been, most probably, inactive for many thousands of years

We assume here that wind power (wind erosion) is the limiting factor for vegetation stability on sand dunes and that dune vegetation can exist only when precipitation is above a minimal threshold of about 50 mm/year (Danin 1996; Tsoar and Blumberg 2002; Tsoar 2005, 2008). Above this value, an increase in precipitation up to ~370 mm/year (Sala et al. 1988) leads to denser vegetation and, therefore, to increased dune stability. When precipitation is above 400 mm/year, the extra water has only a moderate effect on dune vegetation because the plants already have sufficient water to develop. The active dunes of northeastern Brazil, where wind power is very high (Yizhaq et al. 2007, 2009; Tsoar et al. 2009), as well as other coastal dune areas (Hunter et al. 1983; Arens et al. 2004), continue to demonstrate active movement, despite high local rainfall of up to 2 m/year. This fact supports our assumption that precipitation can sometimes have a limited effect on plant growth on sand. Additional supporting evidence that precipitation plays a secondary role in dune activity comes from the northwest Negev desert in Israel. Here, the dunes are stable, despite a very low precipitation rate (between 70 and 170 mm/year) (Karnieli and Tsoar 1995; Meir and Tsoar 1996; Tsoar 2008; Tsoar et al. 2008) because the low wind-drift potential (DP<100) allows the growth of vegetation and biogenic-crust that provide stability (Neuman and Maxwell 1999; Argaman et al. 2006). However, although wind power is the main factor which affects dune mobility, long droughts and drastic decreases in precipitation can lead to dune reactivation or to enhanced dune activity (Lancaster 1997). In addition, in some coastal areas, like Frazer Island in Australia, the sand supply from the ocean may play an additional important role in dune activity. In the work presented below, we mainly focus on the inland large sand seas.

DP is a function of the rate of sand transport (Fryberger 1979; Tsoar 2005), which is given by:

$$\mathrm{DP} = < \mathrm{U}^2 (\mathrm{U} - \mathrm{U_t}) >, \tag{1}$$

where the brackets $\cdots$ indicate time averaging, usually of several years, and U is the wind speed in knots (1 knot=0.514 m/s) at 10 m height. Only wind speeds above the minimal threshold of $\mathrm{U_t}$=12 knots necessary for sand transport are considered, while the weaker winds have zero contribution. Several studies (Fryberger 1979; Bullard 1997) have shown that DP is proportional to the potential sand flux. Fryberger (1979) classified wind energy environments into three categories: (i) low energy with DP<200, (ii) intermediate energy with 200<DP<400, and (iii) high energy with DP>400. Traditionally, the DP calculations are based on annual average tables of specific ranges for wind speed and wind direction. This approach is less accurate than the one given in Eq. (1) due to the rough quantization (and, hence, resolution) of wind speed and direction. It is clear that, in order to obtain a reliable value of DP, wind data with a fine temporal resolution should be used.

The aim of this paper is to verify whether the presently fixed dunes of the Kalahari basin and the Australian dune fields will be reactivated in the future due to global warming, as might be expected from an increase in aridity, which would kill off vegetation. We can accomplish this by: (i) creating a global map of DP derived from measured wind-speed data and two reanalysis databases, and (ii) estimating future DPs using the SRES A1B (see below) climate-change scenario of the Intergovernmental Panel on Climate Change (IPCC) (IPCC 2007). Regions that are more favorable for dune reactivation can then be located. We refrain from quantifying the probability for dune reactivation due to the great uncertainty in extreme wind and precipitation events provided by the IPCC models (see examples below) and because of the complexity of predicting vegetation extinction due to climate change.

Generally speaking, active sand dunes are found in areas where the precipitation rate is very low and/or the DP is relatively large, while stable dunes are found in areas with very low DP and a precipitation rate that is above the minimal threshold of 50 mm/year. Based on this, the results below indicate that the Kalahari stable dunes are not favorable for dune reactivation, primarily because the future DPs will remain very small while the precipitation is predicted to remain significantly above the minimal threshold of 50 mm/year. Most of the Australian stable dune areas are expected to experience an increase in DP and, thus, are more favorable for dune remobilization when compared with the Kalahari dunes, although the probability for dune reactivation in Australia is low.

The paper is organized as follows: First, the data sources that are used in this study are described (Section 2). DP maps, based on measured wind speed and on reanalysis data, are then presented (Sections 3.1, 3.2). Following that, the data of two climate models are used to calculate the future DP and precipitation under the SRES A1B scenario (Section 3.3). Finally, there is a discussion of dune mobility in light of the findings of the climatic models (Section 4), followed by a summary (Section 5).

2 Data sources

The National Climatic Data Center (NCDC; www.ncdc.noaa.gov) provides an hourly database of quality-controlled climate data that includes wind measurements. The database spans a time period from 1900 until the present; the number of stations included in the database generally increases with time, so that the number currently amounts to over 10,000. Unfortunately, most of the stations do not contain sufficiently reliable hourly data, so we chose only those stations that have more than 80% (≈7,013 measurements per year) of reliable hourly wind measurements. We thus could take data from 1,281 stations (distributed globally) for 1973 and 4,984 stations for 2008.

Two reanalysis databases were used for obtaining uniform coverage of the DP— (i) the National Centers for Environmental Prediction, National Center for Atmospheric Research (NCEP/NCAR) (Kalnay et al. 1996) and (ii) the European Centre for Medium-Range Weather Forecasts (ECMWF) ERA40 reanalysis data (Uppala et al. 2005). These two reanalysis databases are intensively used in climate research. The NCEP/NCAR provides reanalysis data from January 1948 until the present (61 years), whereas the ECMWF ERA40 data are provided only from September 1957 to August 2002 (45 years). For the calculation of the DP, we used the finer temporal resolution of these reanalysis data, represented by four values per day (every 6 h), which have a spatial resolution of 2.5° latitude/longitude. Both reanalysis databases provide multilevel coverage of wind velocities, while, for the NCEP/NCAR DP calculation, we used the wind velocities of the lowest level (σ=0.995 where σ is basically the ratio between the atmospheric pressure and surface pressure when assuming that the top of the domain pressure approaches zero), which approximately represents wind at a height of 10 m; for the ECMWF data, we used the 10 m surface winds provided by the model.

For the prediction of future DP levels, we employed the 10 m height wind data of two coupled atmosphere-ocean-general-circulation-models (AOGCMs): (i) the Geophysical Fluid Dynamics Laboratory Climate Model 2.1 (GFDL CM2.1) model (Delworth et al. 2006; Gnanadesikan et al. 2006; Wittenberg et al. 2006; Stouffer et al. 2006) and (ii) the Canadian General Circulation Model version 3.1 (CGCM 3.1). Both are included in the latest IPCC report (IPCC 2007). We used these models because they provide the finest temporal resolution data we could find for daily wind velocities. The atmospheric component of the GFDL model has a spatial resolution of 2° latitude 2.5° longitude, while that of the CGCM is approximately 3.75° latitude/longitude (we used the T47 spectral version of the model). For the prediction of future DP levels, we used the IPCC Special Report on Emissions Scenarios (SRES) A1B scenario runs.[1] We chose the A1B scenario because it seems to represent a moderate global warming scenario (i.e., not too optimistic and not too pessimistic) and because it provides various daily data streams (including wind). To obtain relative changes in DP and precipitation, we compared the model's future predictions with the last part of the IPCC 20th century experiment of these models.

3 Results

3.1 Real data

The NCDC hourly data was used to construct a map of DP distributions. Figure 2 depicts the calculated DP for 2008 (based on 4,984 stations); we use Gaussian smoothing to average several stations that fall on the same grid point. The DP at each grid point (x_0, y_0) is calculated as:

$$\mathrm{DP}(x_0, y_0) = \frac{\sum_{n=1}^{N_p} \overline{\mathrm{DP}}(x_n, y_n) W(x_n, y_n)}{\sum_{n=1}^{N_p} W(x_n, y_n)} \tag{2}$$

where N_p is the number of measured $\overline{\mathrm{DP}}$ points within the "influence region" of the grid point, $\overline{DP}(x_n, y_n)$ is the measured DP; the weighting function $W(x_n, y_n)$ is defined as:

$$W(x_n, y_n) = \exp\left[-(x_n - x_0)^2/X^2 - (y_n - y_0)^2/Y^2\right], \tag{3}$$

using the mapping scales of X=2° and Y=2°. We also assume that the weighting function is zero when $W(x_n, y_n) < e^{-4}$.

Generally speaking, the DP is much larger over the oceans, along coastal areas, and over high mountains. The DP is very small (less than 50) in many inland areas. The locations of the wind stations used to construct the DP map are shown in Fig. 2b. Almost all of them are located in North America, Western Europe, and Japan, making the DP estimation in these areas much more accurate than elsewhere.

Since we are interested in dune areas, we show in Fig. 1 an estimated sand seas map, based on the map of Thomas (1997). The stable sand seas are concentrated in the southern Sahara, Central Asia, Australia, and the Kalahari basin in southern Africa. It is of great interest to predict the future changes in DP and precipitation rates in the stabilized sand seas of Australia and the Kalahari because dune reactivation would affect ecological, economic, and human activity (Knight et al. 2004; Thomas et al. 2005). Because the DP is low for these sand seas and the precipitation is above the rate that is required for vegetative growth,

[1] Quoted from the IPCC report (IPCC 2007): "The A1 storyline and scenario family describes a future world of very rapid economic growth, global population that peaks in mid-century and declines thereafter, and the rapid introduction of new and more efficient technologies. Major underlying themes are convergence among regions, capacity building and increased cultural and social interactions, with a substantial reduction in regional differences in per capita income. The A1 scenario family develops into three groups that describe alternative directions of technological change in the energy system. The three A1 groups are distinguished by their technological emphasis: fossil intensive (A1FI), non-fossil energy sources (A1T), or a balance across all sources (A1B) (where balanced is defined as not relying too heavily on one particular energy source, on the assumption that similar improvement rates apply to all energy supply and end-use technologies)."

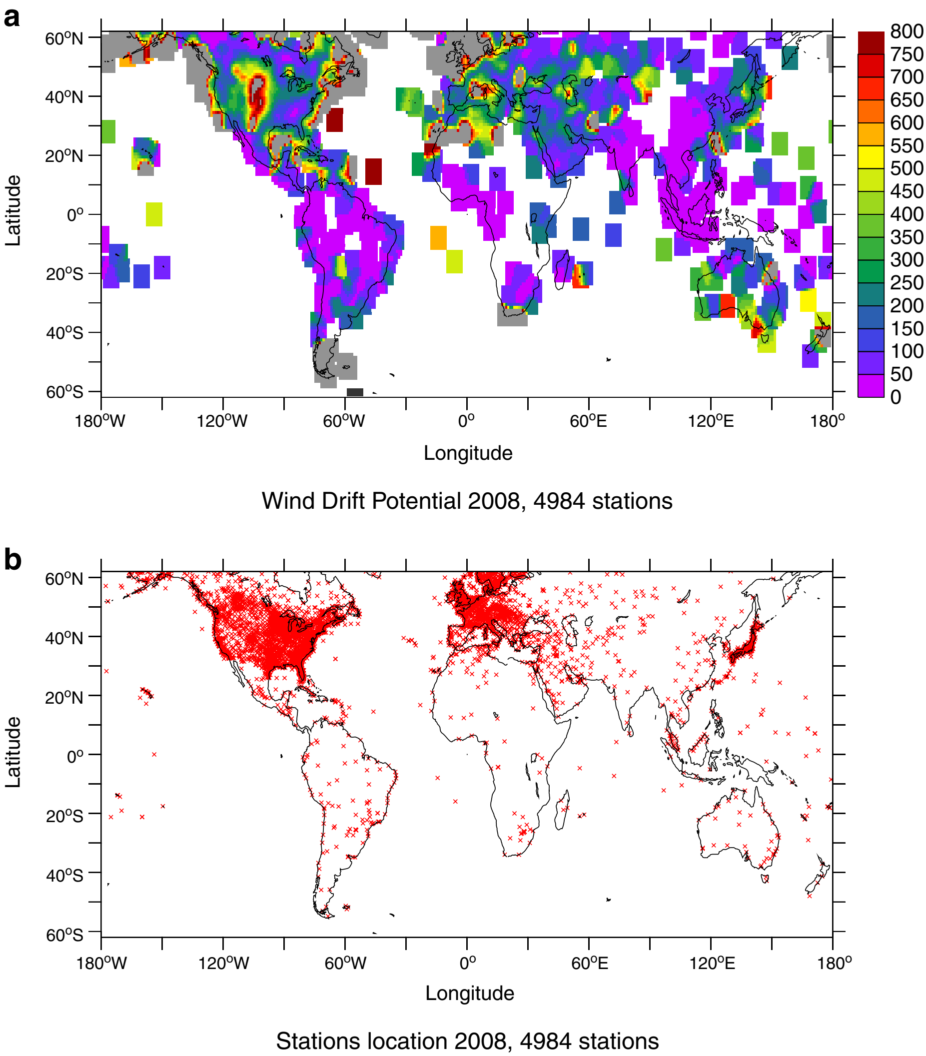

Fig. 2 **a** A global map of the wind drift potential (DP) of 2008. The map was constructed from hourly wind data provided by 4,984 stations of the NCDC. The white color indicates regions with no available data. Gray indicates regions with DP values larger than 800. **b** The distribution of stations used to construct the map in (**a**). Note that the majority of the stations are located in North America, Western Europe, and Japan

perennial vegetation fixes the dunes (Ash and Wasson 1983; Hesse and Simpson 2006; Wiggs et al. 1995). Therefore, we will concentrate on the stable dunes in the Kalahari and Australian deserts.

3.2 Reanalysis data

The surface six-hourly winds of the NCEP/NCAR (Kalnay et al. 1996) and ECMWF (Uppala et al. 2005) reanalysis data were used to obtain a global map of DP distribution (Fig. 3). The DP calculated from the NCEP/NCAR reanalysis for the years 1980–1999

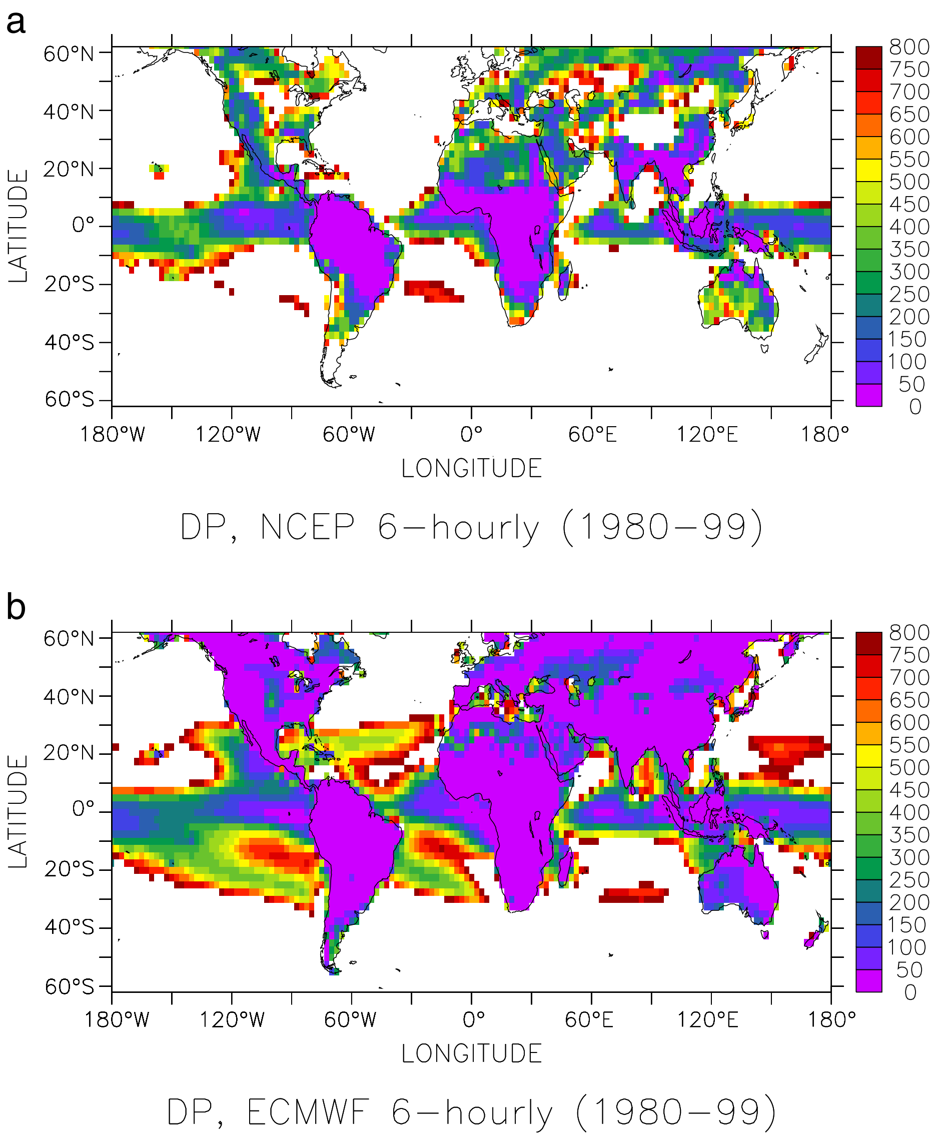

Fig. 3 Global wind drift potential (DP) maps using six-hourly wind speeds from the (**a**) NCEP and (**b**) ECMWF reanalysis data for the 1980–1999 time period. Generally speaking, DPs over the ocean are much larger than over land. The *white* color indicates DP values greater than 800

(Fig. 3a) is generally higher than that of the ECMWF (Fig. 3b). The general features are high DP over the oceans and low DP over the land, similar to the observed data (Fig. 2). For both reanalysis databases, the DP is relatively high over the Sahara and low over the Kalahari basin; this is somewhat similar to the observed values shown in Fig. 2. The reanalysis data is the output of state-of-the-art climate models that assimilate thousands of measurements every 6 h. Thus, at any given time, the reanalysis models should provide a reasonably accurate picture of the climatic state. In essence, DP captures the extreme wind events—stronger winds contribute very significantly to the DP because wind speed appears as a third power factor in Eq. (1). The extreme wind events of the reanalysis data seem to be problematic as reflected in the differences between the DP data calculated from the NCEP/NCAR and ECMWF. We note that the results presented in Fig. 3 are the mean values over 20 years (1980–1999); reanalysis data during this time period are also based on satellite data that provide continuous and high resolution coverage of measurements. The difficulties in calculating consistent, reliable DP values, even from existing reanalysis data that assimilate real data at six-hour intervals, may hint that future predictions of DP from climatic models must be taken with reservations.

To allow a better comparison with climate models that are used for future predictions and for which the finest temporal resolution is daily resolution, we show in Fig. 4 the DP distribution map, based on daily mean values of wind speed; since our main focus in the rest of the paper is the Kalahari and the Australian deserts, we only show the maps of these regions. As expected from the third-power relationship of DP with wind speed, these DP values drop significantly from those calculated from the six-hourly wind data (Fig. 3), although their overall patterns remain similar. Thus, the DP maps that are based on daily mean wind speed provide only the lower limit of the DP, whereas the "real" DPs may be larger. Therefore, comparing daily mean DP maps over

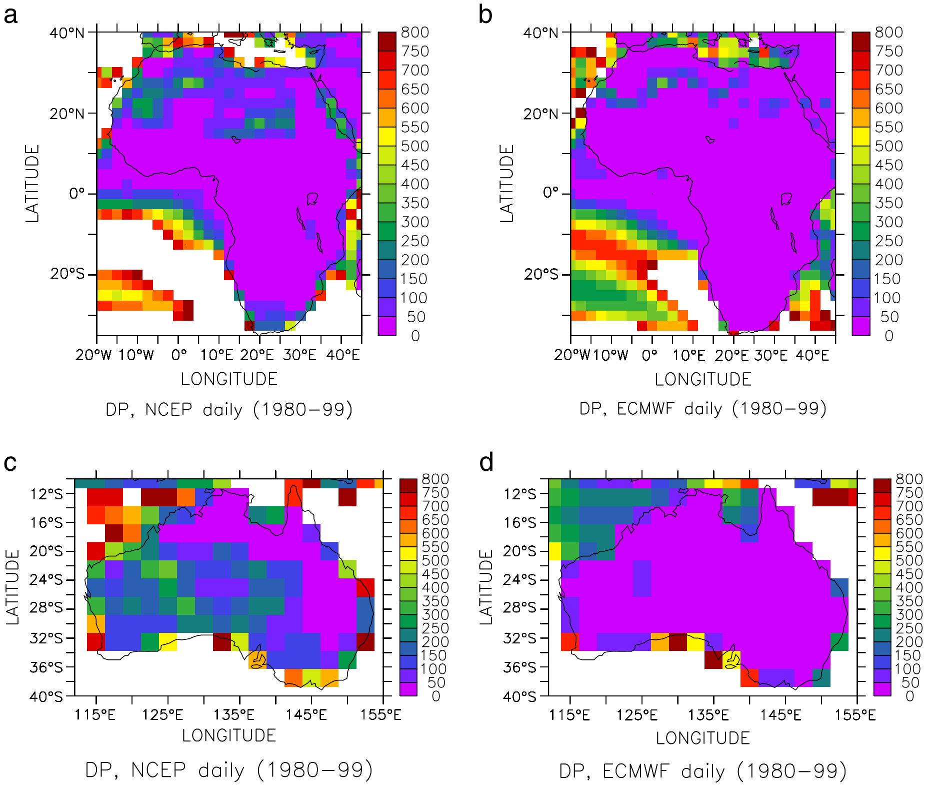

Fig. 4 DP maps that are based on the daily mean wind speed for Africa (*upper panels*) and Australia (*lower panels*) for the NCEP (*left panels*) and ECMWF (*right panels*) reanalysis data for the 1980–1999 time period. DP values that are larger than 800 are marked with a *white* color. Note that the DPs based on the daily mean speed are smaller than those of the six-hourly wind speeds (depicted in Fig. 3)

various periods may help to estimate the relative changes over time, but not necessarily the absolute differences.

To quantify the reduction in DP due to the use of the coarser daily-mean data, we constructed the ratio:

$$r = 1 - \mathrm{DP}_{\mathrm{daily}}/\mathrm{DP}_{6-\mathrm{hourly}}, \tag{4}$$

where $\mathrm{DP}_{6-\mathrm{hourly}}$ indicates DP that is based on six-hourly data and $\mathrm{DP}_{\mathrm{daily}}$ indicates DP based on the coarser daily-mean data. When $\mathrm{DP}_{\mathrm{daily}} = \mathrm{DP}_{6-\mathrm{hourly}}$, $r=0$, indicating a zero reduction in DP due to the daily averaging operation. When $\mathrm{DP}_{\mathrm{daily}}=0$, the ratio is one ($r=1$), meaning a 100% reduction in DP due to the temporal mean. Figure 5 depicts this ratio, showing that the larger reduction is over areas with small DP, while almost zero reduction is observed in many areas over the ocean where the DP is relatively large. The reduction over the Kalahari basin is larger than that of Australia, in part, because the DP over the Kalahari basin is smaller.

Naturally, a comparison between the data (such as in Fig. 2) and the reanalysis data is required to validate the reanalysis model results. Such a comparison is not trivial since the data coverage of the DP maps varies from year to year based on the available data. Yet, when we compare the maps of annual mean DP based on measurements (such as Fig. 2) over the period between 1980 and 1999 to the DP based on the six-hourly reanalysis of NCEP (Fig. 3a) and ECMWF (Fig. 3b), we clearly see that ECMWF provides significantly lower values of the DP data, while NCEP overestimates the DP (mostly in the data coming from North-America, Europe, and Asia). This makes the NCEP DP a more reliable source for wind power analysis as it resembles the measured data more closely.

Vegetation affects dune stability because it increases surface roughness and reduces wind velocity and momentum (Wasson and Nanninga 1986; Buckley 1987; Wolfe and Nickling 1993; Buckley 1996; Hugenholtz and Wolfe 2005). Empirical studies (Danin 1996) have indicated that precipitation between 50 and 100 mm/year can lead to sufficient vegetation cover to reduce dune activity. Vegetation in this low-precipitation range is limited to the interdune areas and the flanks of linear dunes (Danin 1996; Tsoar 1990, 2005; Thomas and Leason 2005); however, biogenic crusts may lead to complete dune fixation even below these low precipitation rates, such as in the Nizzana dunes in the western Negev, Israel (Karnieli and Tsoar 1995).

The vegetation growth rate in sandy soil (as a function of precipitation) increases rapidly up to 370 mm/year (Sala et al. 1988) and more moderately above this value. Once the vegetation cover is extensive and there is more than enough water to saturate the sand, additional precipitation has a smaller effect on plant biomass and cover.

It is thus important to examine contemporary measurements as well as future predictions of precipitation. We compare the precipitation mean rate of 1980–1999 from the NCEP/NCAR and ECMWF reanalysis databases (Fig. 6) and observe that the overall pattern of the two is similar, although there are local differences. Over the dune areas in the Kalahari basin and in Australia, the precipitation rates are several times larger than the minimal threshold of 50 mm/year needed for vegetation growth. Over the Sahara desert, the precipitation rate is below 50 mm/year, which is consistent with the bare, active dunes found in this region. Thus, our main assumption in this work is that full dune reactivation is expected under conditions of a drastic decrease in precipitation (below 50 mm/year) or a drastic increase in DP or from a combination of an increase in DP and a decrease in precipitation (Yizhaq et al. 2009).

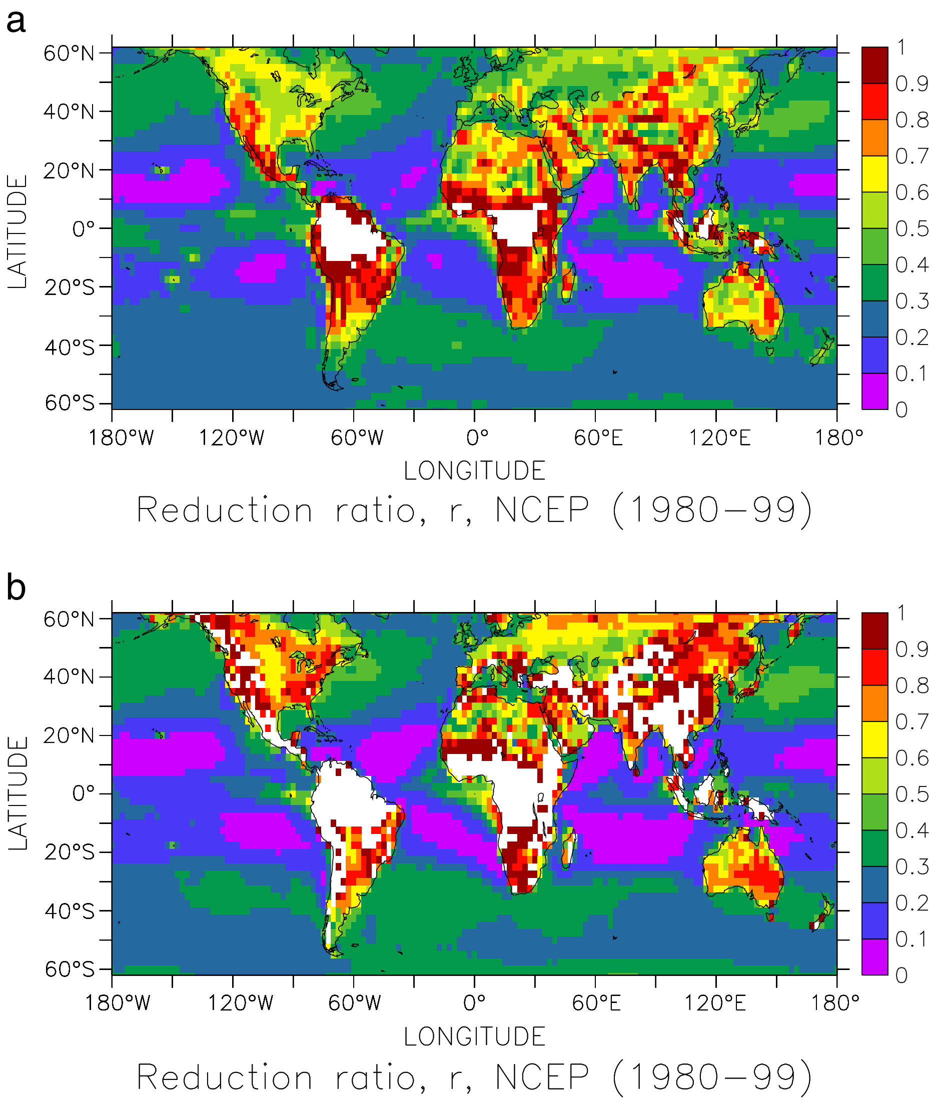

Fig. 5 Same as Fig. 3, but shows the reduction ratio $r=1-DP_{daily}/DP_{6\text{-hourly}}$. The *white* color indicates regions with $DP_{6\text{-hourly}}=0$

3.3 Future predictions

The general circulation models used for long term climate predictions (IPCC 2007) have large uncertainties in predicting climate variables such as wind speeds and precipitation. Climate models running with the same parameters but with different initial conditions can yield different predictions over time due to the "chaotic" nature of the climate system. However, since the results presented here are averaged over several years, the difference between the different initial condition runs becomes much smaller. Still, due to the erratic nature of wind and precipitation and due to the different parametrizations of these fields in

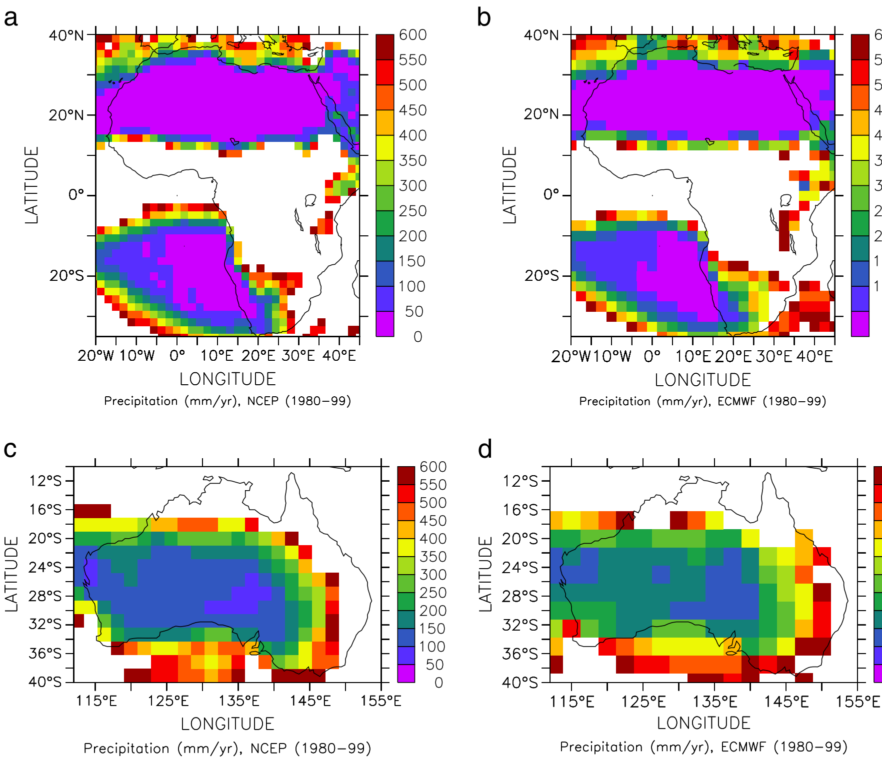

Fig. 6 Precipitation (mm per year) averaged over 1980 to 1999, for Africa (**a**, **b**) and Australia (**c**, **d**) using the NCEP/NCAR (**a**, **c**) and ECMWF ERA40 (**b**, **d**) reanalysis data. Overall, the two reanalysis datasets exhibit similar patterns. The *white* color indicates precipitation greater than 600 mm/year

the different models, a large difference between the models' predictions of DP and precipitation is expected, a difference that increases the uncertainty of the mean predictions. As demonstrated in Figs. 3 and 4, two reanalysis models that should yield similar contemporary DP maps, have large differences, although the overall patterns are similar.

The predictions of DP and precipitation based on the GFDL and CGCM climate models are shown in Figs. 7, 8, 9, 10 and 11. Here, our main interest is the possible future dune reactivation of the fixed dunes of the Kalahari basin and Australian dune fields. Unlike most models, which provide monthly mean wind data, the GFDL and CGCM provide mean wind data on a daily basis, enabling a more reliable estimation of DP. Two representative future periods, 2046–2050 and 2096–2100 were analyzed; we mainly focus on the latter time period. Since we desire to compare future DP and precipitation levels to contemporary values, we use the 1996–2000 data of these models as the baseline.

In Fig. 7 we present the DP of the GFDL and CGCM models calculated for 2096–2100, based on daily mean wind data. The DP values of the GFDL model (Fig. 7a, c) are very low, less than 50 over almost all land areas. The GFDL model-predicted precipitation for the Kalahari region (Fig. 8a, c) is much higher than the minimum threshold for vegetation growth (50 mm/year), and is even higher than the precipitation rate of NCEP/NCAR and ECMWF for 1980–1999, shown in Fig. 6. Over Australia, the precipitation rate is closer to, but still higher than the minimal threshold of precipitation. This suggests that precipitation reduction over Australia, by itself, should not lead to dune reactivation.

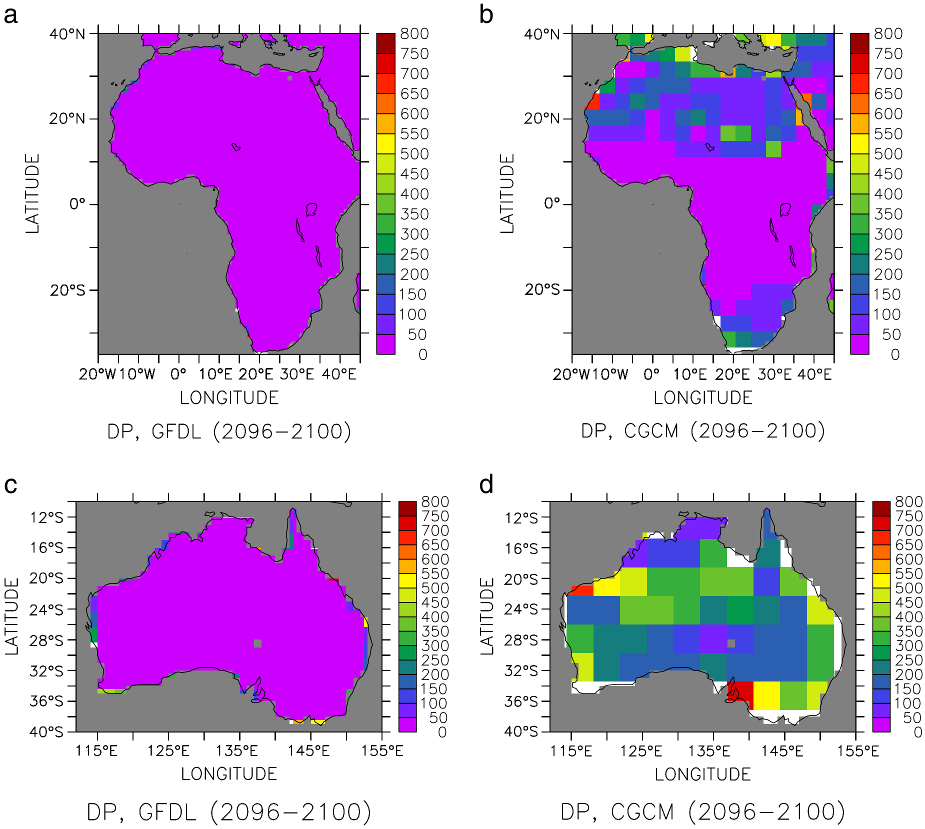

Fig. 7 Prediction of DPs for 2096–2100 for Africa (**a**, **b**) and Australia (**c**, **d**) using the GFDL (**a**, **c**) and CGCM (**b**, **d**) ocean–atmosphere-global-circulation-models. We adopt the models' output of the SRES A1B IPCC scenario

Figures 9 and 10 clearly depict the changes in DP and precipitation between 2096–2100 and 1996–2000, according to the GFDL and CGCM models. As indicated above, the predicted DP calculated in the GFDL model is very small, and thus the difference is also small. However, certain parts of the southern Kalahari basin experience larger predicted DP values. In Australia, the models show that the majority of dunes will have somewhat larger DP values.

The analysis of the CGCM data yields much higher DP values (Fig. 7b, d) than the values of the GFDL (Fig. 7a, c), but closer to the NCEP/NCAR reanalysis data (Fig. 4a, c). Figure 8b, d depicts relatively high precipitation over the Kalahari basin (larger than 500 mm/year) and a more moderate amount (larger than ~250 mm/year) over Australia. Thus, changes in precipitation alone are not expected to cause dune reactivation according to the CGCM. In Figs. 9 and 10, we present the change in DP and precipitation for the years 2096–2100 relative to the 1996–2000 mean according to CGCM model. The DP is predicted to increase over most of Australia, an increase that will increase dune activity. Over Africa, however, the changes in DP are very small, suggesting that the DP will essentially remain at its present value. Precipitation is expected to increase in most areas of Australia and the Kalahari (not shown), except for 2096–2100 for the Kalahari basin

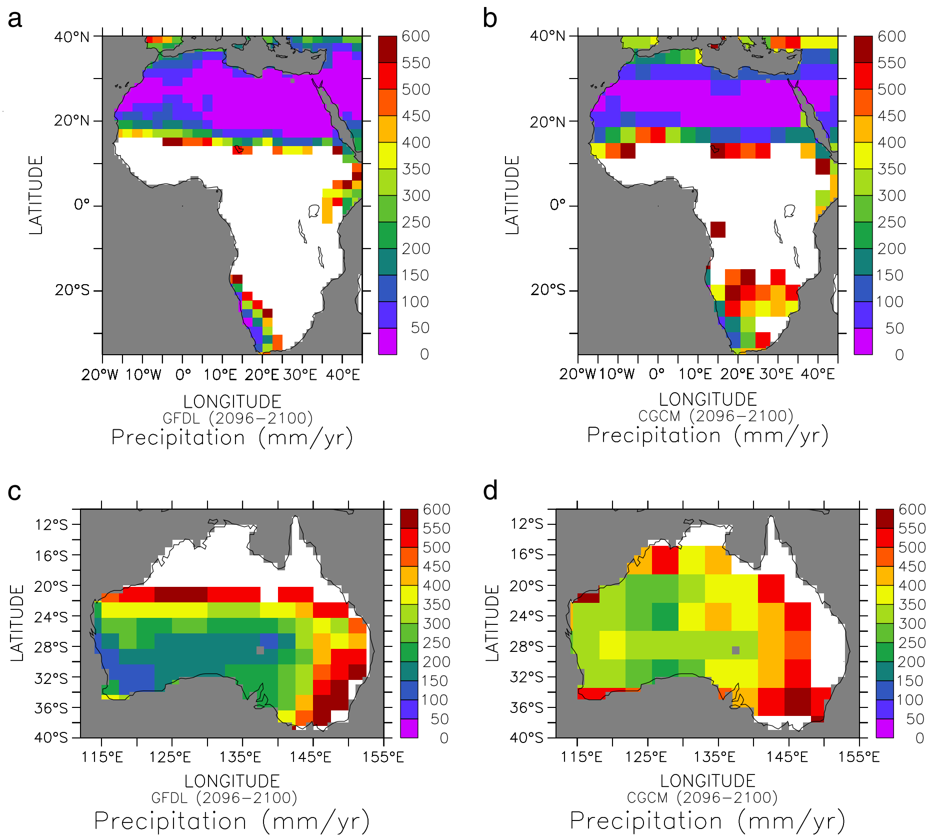

Fig. 8 Same as Fig. 7 for the rate of precipitation (mm/year). The white color indicates precipitation greater than 600 mm/year

(Fig. 10a, b), where there is a predicted decrease in precipitation; yet the precipitation rate is still much higher than the threshold of 50 mm/year.

In Fig. 11 we summarize the DP and precipitation of the different models for the areas in the southern Kalahari and Australian deserts as indicated by the rectangles in Fig. 1; the northern part of the Kalahari is not considered, as it is most probably ancient and very humid. We plotted the DP and precipitation for each of the grid points falling in the selected areas. For the NCEP/NCAR and ECMWF reanalysis data, it is clear that (i) the DP of the Kalahari region is significantly smaller than the DP of the Australian desert and that (ii) the precipitation over the Kalahari region is higher than that over the Australian desert. These observations are consistent with the relatively larger areas of stable dunes in the Kalahari (see Fig. 1). The above observations are also valid for different time periods (1996–2000, 2046–2050, and 2096–2100) of the GFDL and CGCM models. In addition, as indicated above, it is clear that the ECMWF and GFDL models exhibit smaller values of DP, in contrast to the NCEP/NCAR and CGCM. Mean values and standard deviations of the data sets presented in Fig. 11 are given in Table 1.

In recent papers (Yizhaq et al. 2007, 2009), we proposed a model that explains the bi-stability of sand dunes under similar climate conditions. With this model, it is possible to estimate the parameter values (mainly DP and precipitation) for which sand dunes are predicted

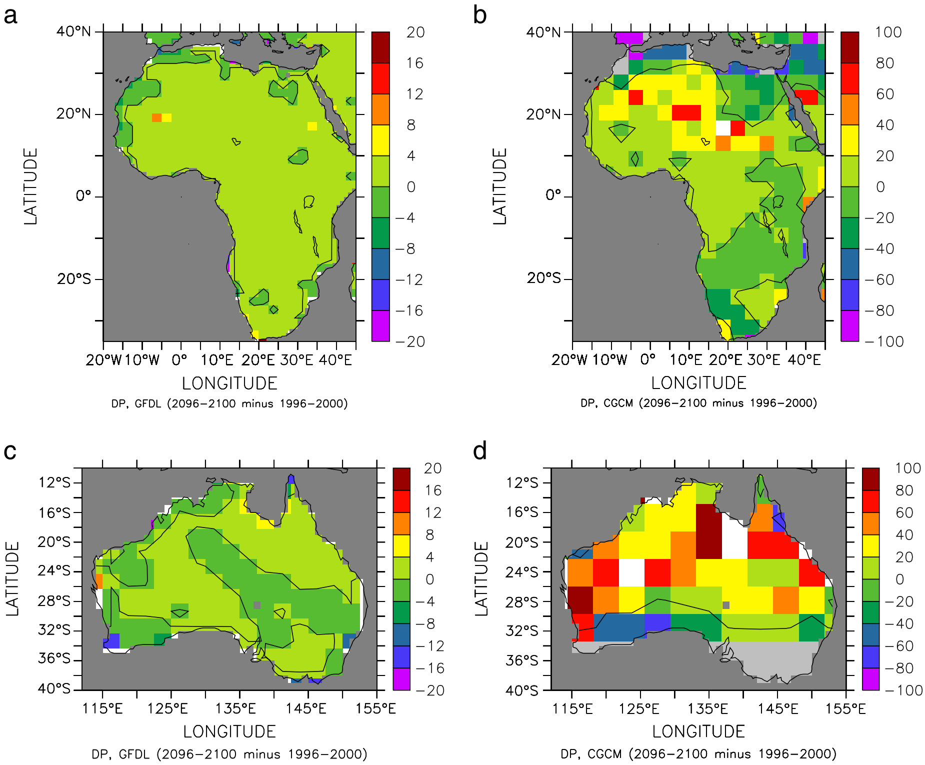

Fig. 9 The differences between the DPs of 2096–2100 and 1996–2000 of the GFDL (**a**, **c**) and CGCM (**b**, **d**) models for Africa (**a**, **b**) and Australia (**c**, **d**). The *solid line* indicates the interpolated zero-contour line. The *white* and *light gray* colors indicate differences that are larger than 100 or smaller than −100, respectively

to be stable (fixed), bi-stable (fixed, active, or both), or active. We indicated these parameter values with solid lines in Fig. 11, and it is apparent that almost all the data points associated with the southern Kalahari and the Australian desert dunes do not fall in the upper zones, indicating active dunes. This is valid both for the present day and for the future. Still, it seems that the Australian desert dunes are more favorable for dune reactivation than those in the Kalahari basin due to the larger predicted increase in DP and the lower predicted amount of precipitation in Australia. Since the changes in DP and precipitation are not drastic (DP is below 400 and the precipitation is above 50 mm/year), it is expected that the Australian fixed dunes will remain stable.

4 Discussion

In order to predict future changes in dune behavior using climate modeling approaches, it is first essential to discuss the main mechanisms that control dune stability/mobility. We assume here that a drastic increase in DP (larger than 400) and a drop in precipitation to below the 50–100 mm/year threshold are most probably necessary (but not sufficient) for reactivating fixed dunes. Active and fixed dunes can coexist with a smaller value of DP and higher values of precipitation as we recently showed (Yizhaq et al. 2009).

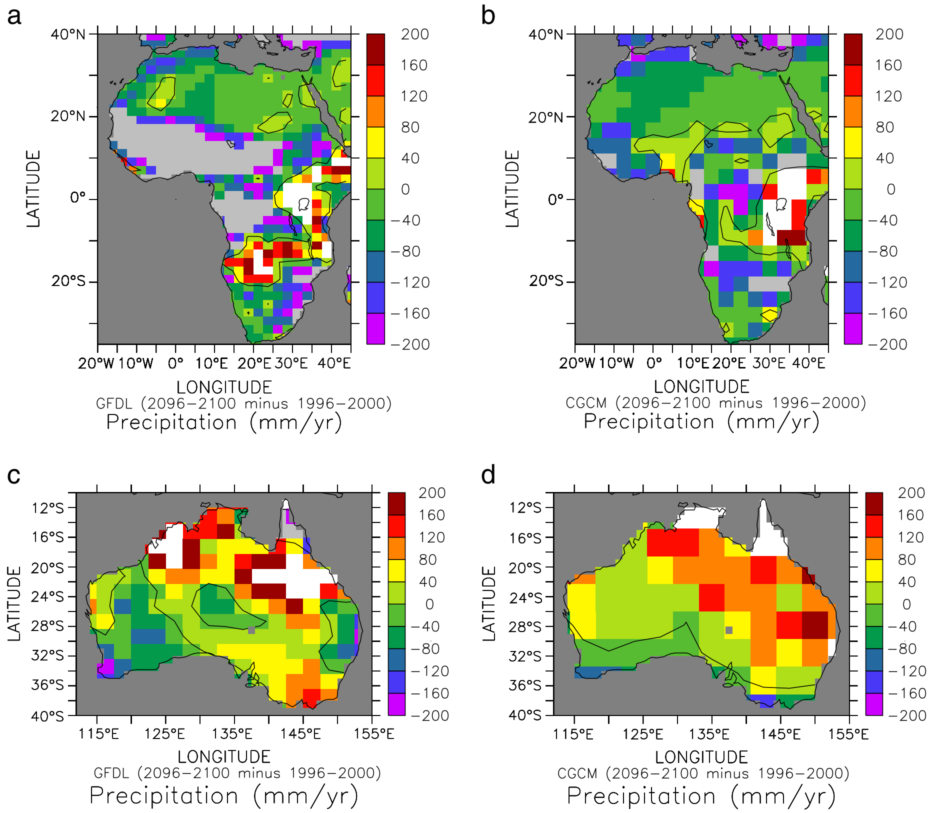

Fig. 10 Same as Fig. 9, for the rate of precipitation (mm/year). The *light gray* color indicates precipitation differences that are smaller than −200 mm/year, while the white color indicates differences that are larger than 200 mm/year

Lancaster (1988) suggested the following dune mobility index:

$$M = W/(P/E_p), \tag{5}$$

where W is the percentage of the time that the wind speed is above the threshold necessary for sand transport, P is the mean precipitation, and E_p is the mean potential evapotranspiration. Large M values indicate dune activity. According to Lancaster (1988), dunes are fully activated for $M>200$, and most dunes are completely stabilized by vegetation for $M<50$. This index was first applied to the Kalahari and was calibrated in other dune fields in South Africa and the USA (Lancaster and Helm 2000). Obviously, the M index is sensitive to a decrease in precipitation since it appears in the denominator of Eq. (5), i.e., when P approaches zero, M diverges. Evapotranspiration can be estimated by Thornthwaite's formula (Thornthwaite 1948), which is based on monthly mean temperatures. As temperature increases, Ep also increases, leading to an increase in the mobility index. Similarly, increasing wind activity (W) also raises the M index. Although Lancaster's formula was applied with success to model dune activity in several dune fields (Muhs and Maat 1993; Lancaster and Helm 2000), there are many counter-examples of active dunes in regions with very high precipitation rates (Yizhaq et al. 2007, 2009; Tsoar et al. 2009), which are characterized by small M values.

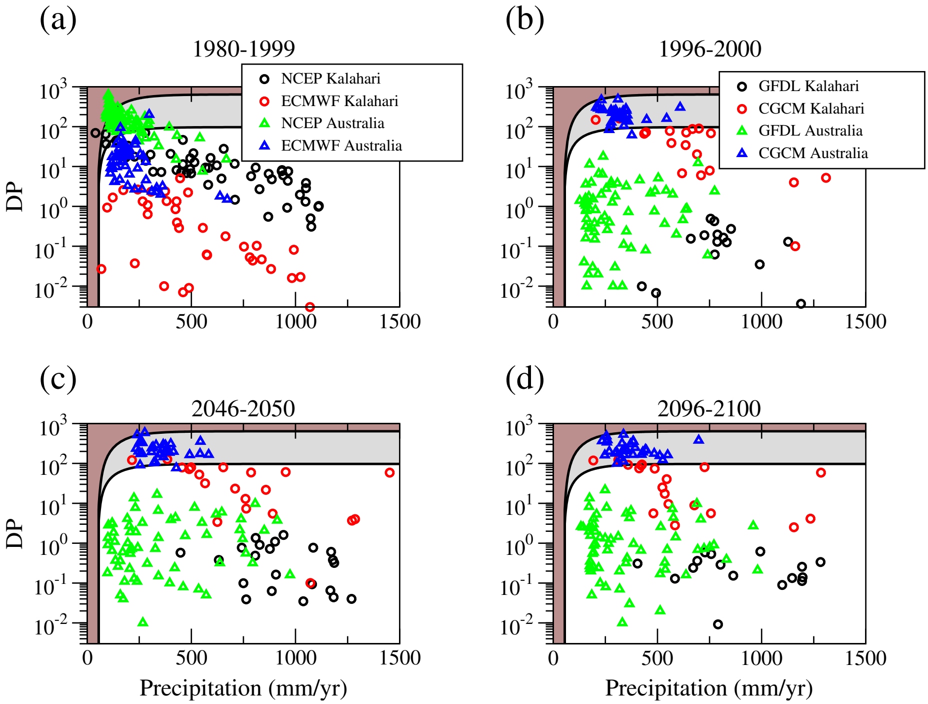

Fig. 11 DP versus precipitation (mm/year) for the different models for the Kalahari (*circles*) and Australian (*triangles*) deserts for the grid points included in the *rectangles* shown in Fig. 1. **a** NCEP/NCAR and ECMWF reanalysis data comparison for the 1980–1999 mean values. **b** GFDL and CGCM models comparison for the time period of 1996–2000. **c** Same as b for years 2046–2050. **d** Same as b for years 2096–2100. The *dark gray* area indicates the DP and precipitation values for which dunes are estimated to be mobile according to Yizhaq et al. (2009); the *light gray* area indicates values for which the dunes can be fixed, active or both, while the *white* area indicates values for which the dunes are estimated to be stable. Note that, since we present DP values that are based on daily mean wind speeds, we have assumed a reduction value of $r=0.7$ [Eq. (4)], typical for the Kalahari and Australian deserts; see Fig. 5

Table 1 Summary of the data presented in Fig. 11; the mean values ±1 std. are given. Note that in many cases the std. of DP is larger than the mean value since DP is a positive value which is stretched toward high values

		Kalahari		Australia	
Dataset	Period	p (mm/year)	DP	p (mm/year)	DP
NCEP	1980–1999	610±320	16±20	179±108	176±116
ECMWF	1980–1999	551±275	0.7±1.1	213±107	21±29
GFDL	1996–2000	929±263	0.06±0.12	308±166	1.8±3.1
	2046–2050	971±290	0.26±0.41	366±230	2.0±3.1
	2096–2100	948±328	0.12±0.17	363±217	2.1±3.5
CGCM	1996–2000	718±296	52±47	323±84	216±95
	2046–2050	761±322	45±40	349±92	237±112
	2096–2100	638±316	46±43	372±102	244±109

Thomas et al. (2005) analyzed GCM data and concluded that most of the dunes in the Kalahari basin are likely to be reactivated by the end of the century. Their prediction is based on a modified "M" index [Eq. (5)] that is basically proportional to the cube of the monthly mean wind speed and inversely proportional to the ratio of precipitation over evapotranspiration; the ratio of winter precipitation and winter evapotranspiration is added to the denominator, thereby weakening the divergence when the monthly precipitation to evapotranspiration ratio approaches zero. Thus, since the worldwide temperature is predicted to increase, including that of Africa, evapotranspiration will also increase and will lead to a larger mobility index, indicating remobilization of the Kalahari basin dunes. Stronger winds and less precipitation may further increase the mobility index. Unlike other mobility indexes, the modified M index resolves monthly changes in dune mobility, which can vary by more than one order of magnitude in the Kalahari. This large seasonal variability is associated with the large seasonality in precipitation and evapotranspiration and also reflects the large sensitivity of this index to changes in precipitation and evapotranspiration. The main purpose in using this modified mobility index was to capture the observed inter-annual variability of sand transport in the Kalahari (Bullard et al. 1996).

There are many issues regarding the use of global circulation models in predicting sand-dune mobility under global warming. Knight et al. (2004) discussed in detail many of these questions and concluded that "in light of this, there appears to be still a long way to go before a comprehensive dune mobility prediction system becomes available." Below we detail some of the factors we believe to be important for dune mobility, but we will not attempt to enter into all the complexities associated with global circulation model performance and dune mobility predictions.

(i). Both the Kalahari basin and the Australian dunes are covered with biogenic, cyanobacterial crusts, up to a few millimeters thick (Thomas and Dougill 2006, 2007; Hesse and Simpson 2006). Our preliminary wind tunnel experiments indicate that biogenic crusts can withstand very strong winds (up to 30 m/s) without experiencing erosion (see also Neuman and Maxwell 1999; Argaman et al. 2006). Moreover, a crust can survive in a dormant mode under drought conditions and return to active growth and development within a few hours after minor rainfall. It is not clear what driving (climatic) forces could erode a biogenic crust and lead to the reactivation of a dune.

(ii). Moreover, even without a biogenic crust, a large DP and/or a very low precipitation rate are necessary to destroy vegetation cover. This is not expected to apply to the Kalahari, where the DP is predicted to remain very low and precipitation to remain high.

(iii). Some mobility indexes are proportional to the cube of the monthly mean wind speed (e.g., Thomas et al. 2005) while the DP, which is directly related to the transported sand, is proportional to the mean of the cube of the wind speed [Eq. (1)]. There is a big difference between the two, and using the cube of the mean wind speed, $\langle U\rangle^3$, to quantify dune mobility instead of the mean of the cube of the wind speed, $\langle U^3\rangle$, may not reflect the future effect of the wind on dune mobility. In Fig. 12, we present the NCEP climatological monthly mean wind speeds as well as the monthly DP values for a grid point in the southwest Kalahari and for a grid point in southwest Australia. While for Australia (Fig. 12b), the seasonal cycle of both mean wind speeds and DPs is similar, for the Kalahari (Fig. 12a), the mean wind speed is at its maximum in August while DP peaks in December. This difference in the timing of the maximum may be attributed, for example, to short, strong storms that drastically increase DP rather than the mean monthly wind speed. Similarly, frequent but weak

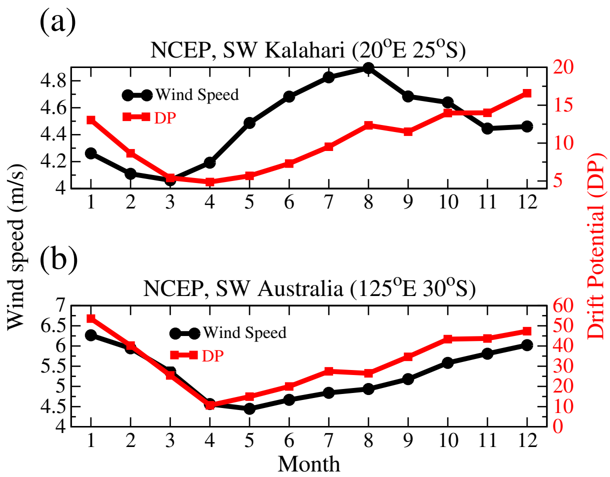

Fig. 12 A comparison between the seasonality of monthly mean wind speeds (*empty circles*) and monthly DP values (*full squares*) for a grid point in the (**a**) southwest Kalahari (20°E 25°S) and (**b**) southwest Australia (125°E 25°S). We used the six-hourly NCEP reanalysis data of the period between 1948 and 2007 to obtain monthly climatological mean values. To obtain the annual DP values, it is necessary to sum the monthly DP values, such that the annual DP for (**a**) is 123 and for (**b**) is 384

winds, caused, for example, by a daily sea-breeze, can drastically increase the monthly mean but not necessarily the DP, leading to a difference in the timing of the maximum value in the annual cycle.

(iv). By definition, the potential evapotranspiration is only a potential. Its real value involves many aspects that relate to plant physiology and not just to meteorological conditions. Real evapotranspiration can be much smaller than the potential, with the relationship between the two most likely a nonlinear one, which must involve various plant-based and environmental factors. Thus, mobility indexes that depend on potential evapotranspiration may exaggerate the drying up process of vegetation. Moreover, in desert areas (such as the Kalahari desert and Australian deserts), perennial vegetation can withstand very prolonged droughts and extreme arid conditions. This point was discussed by Alexander (2007) and raises a challenge to mobility indexes such as those of Lancaster (1988) and Thomas et al. (2005).

(v). Atmosphere-dune interactions may drastically change air temperatures. Specifically, the albedo (the reflection of short-wave solar radiation) is different for biogenic-crust/vegetation (~0.1) and bare sand (~0.4). Thus, when a crust is removed, the surface albedo increases and reflects additional short-wave solar radiation, producing a cooler surface than that covered by a biogenic crust (Oke 1988; Qin et al. 2002, 2005). Surface cooling by several degrees will obviously reduce the actual evapotranspiration and increase the survival of vegetation. This negative feedback tends to preserve vegetation cover even when assuming that the potential evapotranspiration is a major factor that affects dune mobility. This may weaken the effect of increased evapotranspiration under a global warming scenario.

(vi). Under the different global warming scenarios of the IPCC (IPCC 2007), atmospheric CO_2 is expected to continue to increase significantly. As noted by Thomas et al. (2005), this increase will lead to a relative decrease in the opening of vegetation stomata in the vascular plants, since there will be much more CO_2 available for photosynthesis. Thus, the actual evapotranspiration, which occurs through the stomata, will, most likely, be reduced (which could compensate for the increase in evaporation driven by the higher temperatures). This effect is roughly equivalent to a proportional increase in the effective precipitation. It was suggested that, for water-limited systems, the rising of atmospheric CO_2 will increase the vegetation cover of woody species (Donohue et al.

2009). Thus, while an increase in atmospheric CO_2 may lead to warmer conditions and higher potential evapotranspiration, the stomata closing may reduce the actual evapotranspiration, compensating for the effect of the increased temperature.

(vii). Several papers have reported a critical vegetation cover, v_c, below which sand transport is rapidly increased (Wolfe and Nickling 1993; Lee and Soliman 1977; Bullard 1997). v_c is approximately 0.35 for Australia (Ash and Wasson 1983) and 0.14–0.16 for the Kalahari desert (Wiggs et al. 1995; Thomas and Leason 2005). According to this idea, much more drying of vegetation is necessary for sand transport to begin in the Kalahari than in Australia. This makes the Australian dunes more favorable for activation than those in the Kalahari.

These arguments highlight the complexity associated with dune dynamics, and point to the difficulties of using standard climatic models to predict dune remobilization in a quantitative manner. Thus, we can currently provide only qualitative predictions and can only claim, for example, that one region is more likely to undergo dune remobilization than another.

Our estimation of future changes in DP indicates a higher increase in DP values over Australia than over the Kalahari. In addition, the amount of precipitation over the Kalahari will be higher than over Australia. These two estimations make the Australian dunes more likely to reactivate. However, the chances that the Australian dunes will indeed be reactivated are low due to the biogenic crust cover and other factors mentioned above. In addition, the large uncertainties associated with extreme wind events (which are captured by DP) and those associated with precipitation levels further multiply the uncertainties of future predictions of dune mobility. This is reflected by the large deviations between the NCEP/NCAR and ECMWF reanalysis data and the differences between the future predictions of the climate models of GFDL and CGCM.

The majority of the presently stable dunes were active during the last glacial maximum (LGM), about 20,000 years ago. There is much evidence of stronger winds during the LGM than in the Holocene. This is reflected by a higher dust deposition and a greater mobility of sand dunes (Rea 1994; Bigelow et al. 1990; Adams 2003; Harrison et al. 2001; Sarnthein 1978). In addition to the large DP, the global mean precipitation rate was lower during the LGM (e.g., Braconnot et al. 2006). These are ideal conditions for dune activity. The temperature during the LGM was colder; however, this fact is not necessarily associated with less evapotranspiration since the winds were stronger in the LGM. The differences between contemporary conditions and those in the glacial period are very drastic, much more so than the changes predicted to occur as a result of the global warming scenario. In addition, during the warmer period 6,000 years ago, the presently active dunes of the Sahara were stabilized (Sarnthein 1978; Kropelin et al. 2008), most probably due to the higher precipitation of that period. Based on these arguments, we believe that dune reactivation will depend mainly on drastically increased wind power (DP), as well as on a probable decrease in precipitation. Such extreme changes are not expected to occur (according to the GFDL and CGCM models under the SRES A1B scenario) at the end of the 21st century or so, over the Kalahari and Australia, suggesting that the majority of the currently stable dunes will remain stable.

5 Summary

We present a map of DP that is based on the available hourly wind data: high temporal resolution data that may accurately reflect the potential for wind-based sand transport. We then provide global DP maps that are based on six-hourly NCEP/NCAR and ECMWF reanalysis data. These two exhibit differences, reflecting the difficulty in estimating the DP, even with advanced models that assimilate measured data every 6 h. The differences are most likely a result of the difficulties of reanalysis models to reproduce extreme climatic events (and, in particular, extreme wind events). The mean precipitation rates of the two reanalysis models exhibit better congruence. We then analyzed the DP of the future climate in the Kalahari and Australian deserts using the GFDL and CGCM models under the SRES A1B IPCC scenario. The DP predictions of the models are quite different—while the DP of the GFDL model is very low, that of the CGCM is much higher. According to the models, the DP over the Kalahari basin is predicted to remain very low in the future, while major parts over Australia are predicted to have higher DP values. Precipitation predictions show a decrease in vast areas over Australia, bringing the precipitation toward the minimal threshold of ~50 mm/year necessary for vegetation growth. Precipitation decrease is predicted over some regions of the Kalahari dunes, but since the precipitation values are relatively high, this decrease is not expected to lead to major vegetation extinction. The main conclusion of our study is that, under the global warming scenario SRES A1B, both the Kalahari and Australian dunes have a low probability to be reactivated, though the Australian dunes have a higher probability to undergo remobilization than those of the Kalahari.

Acknowledgements We thank the Israeli Science Foundation and the Israeli Ministry for Environmental Protection for financial support. We thank Nafatali Lazarovitch and Eli Zaady for helpful discussions and Shai Kaplan for construction of the dune-field map (Fig. 1).

References

Adams KD (2003) Estimating palaeowind strength from beach deposits. Sedimentology 50:565–577

Alexander WRG (2007) Locally-developed climate model verified. Water Wheel 6(1):27–29

Arens SM, Slings Q, de Vries CN (2004) Mobility of a remobilised parabolic dune in Kennemerland, The Netherlands. Geomorphology 59(1–4):175–188

Argaman E, Singer A, Tsoar H (2006) Erodibility of some crust forming soils/sediments from the Southern Aral Sea Basin as determined in a wind tunnel. Earth Surf Process Landf 31:47–63

Ash JE, Wasson RJ (1983) Vegetation and sand mobility in the Australian desert dunefield. Z Geomorphol 45:7–25

Bigelow N, Beget J, Powers R (1990) Latest Pleistocene increase in wind intensity recorded in eolian sediments from central Alaska. Quat Res 34:160–168

Braconnot P, Otto-Bliesner B, Harrison S, Joussaume S, Peterchmitt J-Y, Abe-Ouchi A, Crucifix M, Fichefet T, Hewitt CD, Kageyama M, Kitoh A, Loutre M-F, Marti O, Merkel U, Ramstein G, Valdes P, Weber L, Yu Y, Zhao Y (2006) Coupled simulations of the mid-Holocene and Last Glacial Maximum: new results from PMIP2. Clim Past Discuss 2(6):1293–1346. URL http://www.clim-past-discuss.net/2/1293/2006/

Buckley R (1987) The effect of sparse vegetation on the transport of dune sand by wind. Nature 325:426–428

Buckley R (1996) Effects of vegetation on the transport of dune sand. Ann Arid Zone 35(3):215–223

Bullard JE (1997) A note on the use of the "Fryberger method" for evaluating potential sand transport by wind. J Sediment Res 67(3):499–501

Bullard JE, Thomas DSG, Livingstone I, Wiggs GFS (1996) Wind energy variations in the southwestern Kalahari desert and implications for linear dunefield activity. Earth Surf Process Landf 21(3):263–278

Danin A (1996) Plants of desert dunes. Springer, Berlin

Delworth TL, Broccoli AJ, Rosati A, Stouffer RJ, Balaji V, Beesley JA, Cooke WF, Dixon KW, Dunne J, Dunne KA, Durachta JW, Findell KL, Ginoux P, Gnanadesikan A, Gordon CT, Griffies SM, Gudgel R, Harrison MJ, Held IM, Hemler RS, Horowitz LW, Klein SA, Knutson TR, Kushner PJ, Langenhorst AR, Lee HC, Lin SJ, Lu J, Malyshev SL, Milly PCD, Ramaswamy V, Russell J, Schwarzkopf MD, Shevliakova E, Sirutis JJ, Spelman MJ, Stern WF, Winton M, Wittenberg AT, Wyman B, Zeng F, Zhang

R (2006) GFDL's CM2 global coupled climate models. Part I: formulation and simulation characteristics. J Clim 19(5):643–674

Donohue RJ, McVicar TR, Rederick ML (2009) Climate-related trends in Australian vegetation cover as inferred from satellite observations, 1981–2006. Glob Chang Biol 15:1025–1039

Duller GAT, Augustinus PC (2006) Reassessment of the record of linear dune activity in Tasmania using optical dating. Quat Sci Rev 25(19–20):2608–2618

Fitzsimmons KE, Bowler JM, Rhodes EJ, Magee JM (2007a) Relationships between desert dunes during the late quaternary in the Lake Frome region, Strzelecki Desert, Australia. J Quat Sci 22(5):549–558

Fitzsimmons KE, Rhodes EJ, Magee JW, Barrows TT (2007b) The timing of linear dune activity in the Strzelecki and Tirari Deserts, Australia. Quat Sci Rev 26(19–21):2598–2616

Fryberger SG (1979) Dune forms and wind regime. In: McKee ED (ed) A study of global sand seas. Vol. 1052. U.S. Geol. Surv., pp. 137–169

Gnanadesikan A, Dixon KW, Griffies SM, Balaji V, Barreiro M, Beesley JA, Cooke WF, Delworth TL, Gerdes R, Harrison MJ, Held IM, Hurlin WJ, Lee HC, Liang Z, Nong G, Pacanowski RC, Rosati A, Russell J, Samuels BL, Song Q, Spelman MJ, Stouffer RJ, Sweeney CO, Vecchi G, Winton M, Wittenberg AT, Zeng F, Zhang R, Dunne JP (2006) GFDL's CM2 global coupled climate models. Part II: The baseline ocean simulation. J Clim 19(5):675–697

Harrison SP, Kohfeld KE, Roelandt C, Claquin T (2001) The role of dust in climate changes today, at the last glacial maximum and in the future. Earth Sci Rev\ 54(1–3):43–80

Hesse PP, Simpson RL (2006) Variable vegetation cover and episodic sand movement on longitudinal desert sand dunes. Geomorphology 81:276–291

Hesse PP, Humphreys GS, Selkirk PM, Adamson DA, Gore DB, Nobes DC, Price DM, Schwenninger JL, Smith B, Tulau M, Hemmings F (2003) Late Quaternary aeolian dunes on the presently humid Blue Mountains, Eastern Australia. Quat Intertropical 108:13–32

Hugenholtz CH, Wolfe SA (2005) Biogeomorphic model of dunefield activation and stabilization on the northern Great Plains. Geomorphology 70(1–2):53–70

Hunter RE, Richmond BM, Alpha TR (1983) Storm-controlled oblique dunes of the Oregon coast. Geol Soc Am Bull 94(12):1450–1465

IPCC (2007) Climate change 2007: the physical science basis. Contribution of working group I to the fourth assessment report of the intergovernmental panel on climate change. Cambridge University Press, Cambridge, United Kingdom and New York, NY, USA

Kalnay E, Kanamitsu M, Kistler R, Collins W, Deaven D, Gandin L, Iredell M, Saha S, White G, Woollen J, Zhu Y, Chelliah M, Ebisuzaki W, Higgins W, Janowiak J, Mo KC, Ropelewski C, Wang J, Leetmaa A, Reynolds R, Jenne R, Joseph D (1996) The NCEP/NCAR 40-year reanalysis pro ject. Bull Am Meteorol Soc 77(3):437–471

Karnieli A, Tsoar H (1995) Spectral reflectance of biogenic crust developed on desert dune sand along the Israel-Egypt border. Int J Remote Sens 16(2):369–374

Knight M, Thomas DSG, Wiggs GFS (2004) Challenges of calculating dunefield mobility over the 21st century. Geomorphology 59:197–213

Kropelin S, Verschuren D, Lezine AM, Eggermont H, Cocquyt C, Francus P, Cazet J-P, Fagot M, Rumes B, Russell J, Darius F, Conley DJ, Schuster M, Suchodoletz HV, Engstrom DR (2008) Climate-driven ecosystem succession in the Sahara: the past 6000 years. Science 320:765–768

Lancaster N (1988) Development of linear dunes in the southwestern Kalahari, Southern Africa. J Arid Environ 14:233–244

Lancaster N (1997) Response of eolian geomorphic systems to minor climate change: examples from the southern Californian deserts. Geomorphology 19:333–347

Lancaster N, Helm K (2000) A test of a climatic index of dune mobility using measurements from the southwestern United States. Earth Surf Proc Landf 25:197–207

Lee BE, Soliman BF (1977) An investigation of the forces on three dimensional bluff bodies in rough wall turbalent boundary layers. Transact ASME, J Fluid Eng 99(3):503–510

Lunt DJ, Valdes PJ (2001) Dust transport to Dome C, Antarctica, at the Last Glacial Maximum and present day. Geophys Res Lett 28(2):295–298

Lunt DJ, Valdes PJ (2002) Dust deposition and provenance at the Last Glacial Maximum and present day. Geophys Res Lett 29(22):2085

Meir A, Tsoar H (1996) International borders and range ecology: the case of Bedouin transborder grazing. Hum Ecol 24(1):39–64

Muhs DR, Maat PB (1993) The potential response of eolian sands to greenhouse warming and precipitation reduction on the Great Plains of the USA. J Arid Environ 25:905–918

Neuman CM, Maxwell C (1999) A wind tunnel study of the resilience of three fungal crusts to particle abrasion during aeolian sediment transport. Catena 38(2):151–173

Oke TR (1988) Boundary layer climates. Methuen, London

Okin GS (2008) A new model of wind erosion in the presence of vegetation. J Geophys Res Earth Surf 113: F02S10

Qin Z, Berliner PR, Karnieli A (2002) Remote sensing analysis of the land surface temperature anomaly in the sand-dune region across the Israel-Egypt border. Int J Remore Sens 23(19):3991–4018

Qin Z, Berliner PR, Karnieli A (2005) Ground temperature measurement and emissivity determination to understand the thermal anomaly and its significance on the development of an arid environmental ecosystem in the sand dunes across the Israel-Egypt border. J Arid Environ 60(1):27–52

Rea DK (1994) The paleoclimatic record provided by eolian deposition in the deep-sea—the geologic history of wind. Rev Geophys 32:159–195

Sala OE, Parton WJ, Joyce LA, Lauenroth WK (1988) Primary production of the central grassland region of the United-States. Ecology 69(1):40–45

Sarnthein M (1978) Sand deserts during glacial maximum and climatic optimum. Nature 272:43–46

Stone AEC, Thomas DSG (2008) Linear dune accumulation chronologies from the southwest Kalahari, Namibia: challenges of reconstructing late Quaternary palaeoenvironments from aeolian landforms. Quat Sci Rev 27:1667–1681

Stouffer RJ, Broccoli AJ, Delworth TL, Dixon KW, Gudgel R, Held I, Hemler R, Knutson T, Lee HC, Schwarzkopf MD, Soden B, Spelman MJ, Winton M, Zeng F (2006) GFDL's CM2 global coupled climate models. Part IV: idealized climate response. J Clim 19(5):723–740

Talbot MR (1984) Late Pleistocene rainfall and dune building in the Sahel. Palaeoecol Afr 16:203–214

Thomas DSG (1997) Arid zone geomorphology. Wiley, New-York, Ch. Sand seas and aeolian bedforms, pp. 373–412

Thomas AD, Dougill AJ (2006) Distribution and characteristics of cyanobacterial soil crusts in the Molopo Basin, Southern Africa. J Arid Environ 64:270–283

Thomas AD, Dougill AJ (2007) Spatial and temporal distribution of cyanobacterial soil crusts in the Kalahari: implications for soil surface properties. Geomorphology 85:17–29

Thomas DSG, Leason HC (2005) Dunefield activity response to climate change in the southwest Kalahari. Geomorphology 64:117–132

Thomas DSG, Knight M, Wiggs GFS (2005) Remobilization of southern African desert dune systems by twenty-first century global warming. Nature 435:1218–1221

Thornthwaite CW (1948) An approach toward a rational classification of climate. Geogr Rev 38:55–94

Tsoar H (1990) The ecological background, deterioration and reclamation of desert dune sand. Agric Ecosyst Environ 33:147–170

Tsoar H (2005) Sand dunes mobility and stability in relation to climate. Phys A 357(1):50–56

Tsoar H (2008) Land use and its effect on the mobilization and stabilization of the NW Negev sand dunes. In: Breckle SW, Yair A, Veste M (eds) Arid dune ecosystems of ecological studies. Vol. 200 of Ecological Studies. Springer, Berlin, pp 79–90

Tsoar H, Blumberg DG (2002) Formation of parabolic dunes from barchan and transverse dunes along Israel's Mediterranean coast. Earth Surf Process Landf 27(11):1147–1161

Tsoar H, Blumberg DG, Wenkart R (2008) Formation and geomorphology of the NW Negev sand dunes. In: Breckle SW, Yair A, Veste M (eds) Arid dune ecosystems. Vol. 200 of Ecological Studies. Springer, pp. 25–48

Tsoar H, Levin N, Porat N, Maia L, Herrmann H, Tatumi SH, Sales VC (2009) The effect of climate change on the mobility and stability of coastal sand dunes in Ceará State (NE Brazil). Quat Res 71(2):217–226

Uppala SM, Kallberg PW, Simmons AJ, Andrae U, da Costa Bechtold V, Fiorino M, Gibson JK, Haseler J, Hernandez A, Kelly GA, Li X, Onogi K, Saarinen S, Sokka N, Allan RP, Andersson E, Arpe K, Balmaseda MA, Beljaars ACM, van de Berg L, Bidlot J, Bormann N, Caires S, Chevallier F, Dethof A, Dragosavac M, Fisher M, Fuentes M, Hagemann S, Holm E, Hoskins BJ, Isaksen L, Janssen PAEM, Jenne R, McNally A, Mahfouf J-F, Morcrette J-J, Rayner NA, Saunders RW, Simon P, Sterl A, Trenberth KE, Untch A, Vasiljevic D, Viterbo P, Woollen J (2005) The ERA-40 reanalysis. Quart J Roy Meteor Soc 131:2961–3012

Wasson RJ (1984) Late Quaternary palaeoenvironments in the desert dunefields of Australia. In: Vogel JC (ed) Late Cainozoic Palaeoclimates of the Southern Hemisphere. A. A. Balkema, Rotterdam, pp 419–432

Wasson RJ, Nanninga PM (1986) Estimating wind transport of sand on vegetated surfaces. Earth Surf Process Landf 11(55):505–514

Wiggs GFS, Livingstone I, Thomas DSG, Bullard JE (1995) Dune mobility and vegetation cover in the Southwest Kalahari Desert. Earth Surf Process Landf 20:515–530

Wittenberg AT, Rosati A, Lau NC, Ploshay JJ (2006) GFDL's CM2 global coupled climate models. Part III: tropical pacific climate and ENSO. J Clim 19(5):698–722

Wolfe SA, Nickling WC (1993) The protective role of sparse vegetation in wind erosion. Prog Phys Geog 17:50–68

Yizhaq H, Ashkenazy Y, Tsoar H (2007) Why do active and stabilized dunes coexist under the same climatic conditions? Phys Rev Lett 98:188001

Yizhaq H, Ashkenazy Y, Tsoar H (2009) Sand dune dynamics and climate change: a modeling approach. J Geophys Res 114:F01023